Proceedings of the European Conference Physics of Magnetism, Poznań 2014

Magnetic Properties of $CeNi_4Mn_yAl_{1-y}$ Compounds

K. Synoradzki* and T. Toliński

Institute of Molecular Physics, Polish Academy of Sciences, M. Smoluchowskiego 17, 60-179 Poznań, Poland

The magnetic properties of the polycrystalline $CeNi_4Mn_yAl_{1-y}$ compounds have been investigated combining AC susceptibility, field-cooled and zero-field-cooled DC magnetization and magnetic relaxation measurements. The X-ray diffraction measurements showed that the group $CeNi_4Mn_yAl_{1-y}$ is isostructural and crystallizes in the $CaCu_5$-type structure ($P6/mmm$). For $0 < y < 1$ irreversible magnetism, long-time magnetic relaxation effect and evident upshift of the AC susceptibility peak with increasing frequency are observed at low temperatures. The spin-glass-like behaviour originates from disorder due to the statistical occupation of the 3g site. Using our data we have constructed the tentative phase diagram.

DOI: 10.12693/APhysPolA.127.210

PACS: 75.50.Lk, 71.20.Lp

1. Introduction

Cerium based intermetallic compounds are demonstrative examples of systems with strong electron correlations. They exhibit fascinating effects like: effective mass enhancement (heavy fermions — HF), fluctuating valence (FV), Kondo effect, Kondo lattices (KL) formation, superconductivity, ferromagnetism (FM), spin-glass (SG) behaviour, etc.

Our interest was attracted by the $CeNi_4Al$–$CeNi_4Mn$ isostructural systems due to a possible valence transition and the interplay between $3d$ and $4f$ magnetism. The $CeNi_4Mn$ compound is a soft ferromagnet with $T_C \approx 130$ K and a stable Ce^{+3} valence, whereas in $CeNi_4Al$ FV has been observed.

Although many studies have been carried out on Ce based materials in which the Ce ions are in non-magnetic host environments, very little work has been done on materials in which the Ce ions are embedded in robust internal host magnetic fields [1]. Moreover, the substitution of Mn by Al is rather rare.

In this paper, we report for the first time the magnetic properties and we focus on characterization and discussion of the diluted magnetic system of the Mn-doped $CeNi_4Al$ ($0 < y < 1$).

2. Experimental details

Polycrystalline samples were prepared by induction melting of stoichiometric amounts of pure elements in the argon atmosphere. The samples were turned and remelted several times to achieve a better homogeneity.

The crystal structure was established by a powder X-ray diffraction (XRD) technique, using Co K_α radiation. The full-pattern Rietveld refinement using FullProf has confirmed the hexagonal $CaCu_5$-type structure ($P6/mmm$ space group) for all the prepared samples. Ce occupies the 1a site (0, 0, 0) and Ni(1) the 2c site (1/3, 2/3, 0). Ni(2), Al and Mn are statistically distributed over the 3g sites (1/2, 0, 1/2).

The DC and AC magnetic susceptibility were measured in the temperature range 2–300 K using the PPMS (Quantum Design) commercial device.

3. Results

The XRD patterns revealed that all samples show essentially a single phase. Figure 1 presents an exemplary XRD pattern for the $CeNi_4Mn_{0.7}Al_{0.3}$ sample recorded at room temperature. The obtained lattice parameters decrease with the Mn content (not shown here). The Vegard law is not strictly obeyed, which may stem from the valence variation of the Ce and/or Mn atoms. Additionally, the strain energy, the stress field or the compressibility of the components could result in the deviations from the Vegard law. Such variation of lattice parameters are often observed in similar systems [2, 3].

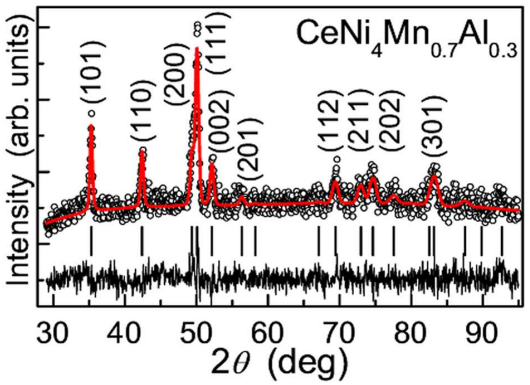

Fig. 1. X-ray diffraction pattern along with the fitting curve for the $CeNi_4Mn_{0.7}Al_{0.3}$ sample. The bottom solid line shows the difference between the measured and the calculated patterns. The vertical bars indicate the positions of the structural reflections.

Figure 2 shows the temperature dependence of the zero field cooled (ZFC) magnetization normalized to the maximum value for each sample. There is a peak for all Mn and Al containing samples, which moves to higher temperature with the Mn concentration. For the sample with $y = 0.1$ the peak is out of temperature range.

*corresponding author; e-mail: karol.synoradzki@ifmpan.poznan.pl

As can be seen in Fig. 3 the peak of χ_{DC} becomes broader and moves to lower temperatures while increasing the strength of the magnetic field. Moreover, a comparison of the ZFC and FC curves reveals a strong irreversibility (Fig. 3). Such magnetic behaviour is observed in many SG systems. Above the peaks, samples are paramagnetic (PM) and the magnetic susceptibility curves can be fitted with the Curie–Weiss formula (not shown here).

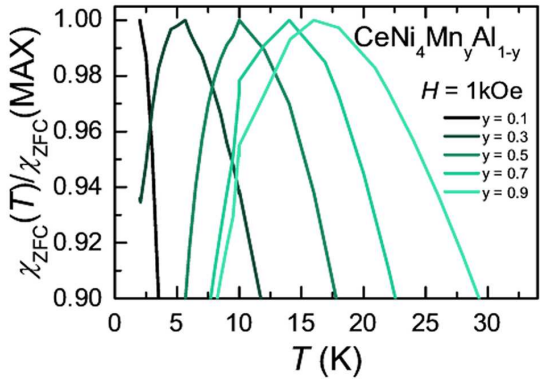

Fig. 2. Temperature dependence (ZFC mode) of the normalized DC magnetization curves for $CeNi_4Mn_yAl_{1-y}$ as a function of y. The applied magnetic field was equal to 1 kOe.

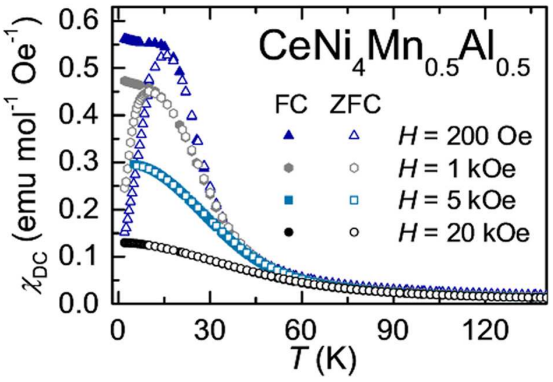

Fig. 3. Temperature variation of the DC magnetization of the $CeNi_4Mn_{0.5}Al_{0.5}$ alloy in the ZFC and FC modes.

The field variation of the magnetizations taken at 2 K are presented in Fig. 4. For all Mn and Al containing samples a hysteresis was observed. One cannot see a complete saturation of magnetization even at high fields for any compositions, which is often observed in SG systems.

In order to confirm the SG effect, we performed an AC susceptibility χ_{AC} measurement at the frequency range 10 Hz $\leq \omega/2\pi \leq$ 10 kHz with an AC field $H_{AC} = 5$ Oe. Figure 5 shows real χ' and imaginary χ'' part of χ_{AC} for $CeNi_4Mn_{0.5}Al_{0.5}$ alloy as an example. The position of the cusp in χ' and χ'' is frequency-dependent, shifting to higher temperatures at higher frequencies. This behaviour can be described by the empirical Vogel–Fulcher (V-F) law, $f = f_0 \exp(-E_a/k_B(T_f - T_0))$, with two fitting parameters:

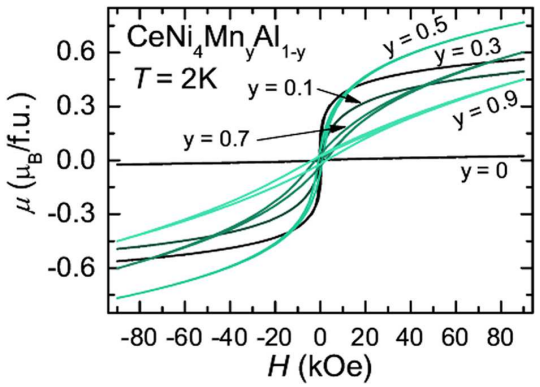

Fig. 4. Isothermal magnetization vs. magnetic field up to 90 kOe measured at 2 K for the $CeNi_4Mn_yAl_{1-y}$ alloys.

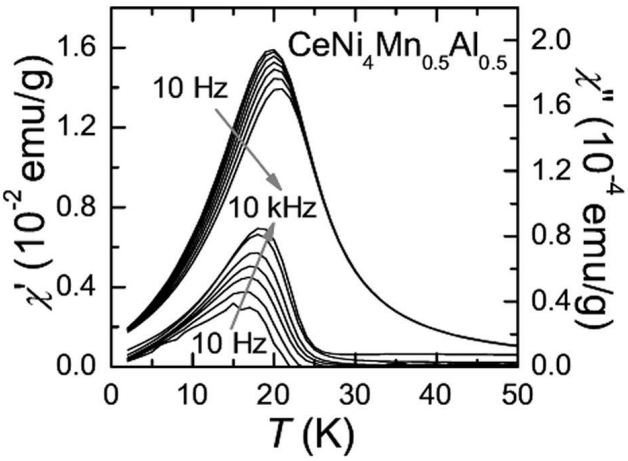

Fig. 5. Temperature and frequency dependence of the real (top, left y-axis) and imaginary (down, right y-axis) part of the AC magnetization of $CeNi_4Mn_{0.5}Al_{0.5}$.

V–F temperature T_0 and activation energy E_a. f_0 is a characteristic frequency fixed as 10^{13} Hz.

The plot of T_f as a function of $1/\ln(f_0/f)$ is displayed in Fig. 6a. Additionally, we have used the dynamical slowing down expression, $\tau/\tau_0 = [(T_f/T_g) - 1]^{zv}$, to describe the frequency dependence, where $\tau = 1/2\pi f$, τ_0 is the relaxation time related to f_0, T_g is the spin-glass temperature and zv is the critical exponent, which is in the range 4–12 for SG. From Fig. 6b it is clear that this relation is obeyed. Using the analysis method mentioned above, the values of characteristic parameters were estimated for all Mn and Al containing samples and all of them fall in the values range typical of SG materials.

The presence of magnetic glassy state is often characterized by the presence of time-dependent remanent magnetism. Unlike a permanent magnet, the magnetization of SG materials decreases fast within a relatively short period. Time dependence of normalized magnetization at 2 K after cooling the sample without magnetic field is shown in Fig. 7. For all Mn and Al containing samples the change of magnetization in time shows similar behaviour. Using a function, $M(T, t) =$

$M_0(T,\,0)+\alpha(T)\ln(t+t_s)+\beta\exp((-t+t_s)/\tau)$, the $M(t)$ data can been fitted very well over the full time range studied. $M_0(T)$, τ, t_s, α and β are fitting parameters.

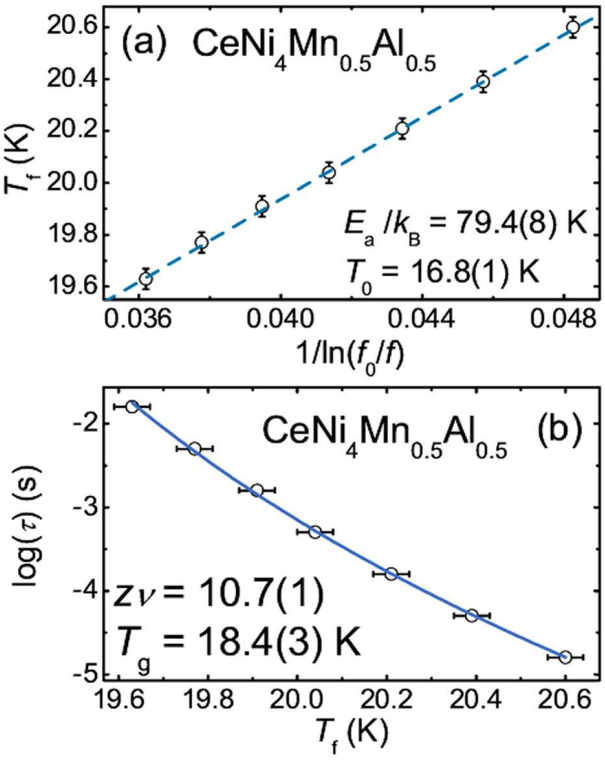

Fig. 6. Frequency dependence of spin freezing temperature T_f for $CeNi_4Mn_{0.5}Al_{0.5}$ plotted as (a) T_f vs. $1/\ln(f_0/f)$ and (b) $\log(\tau)$ vs. T_f. The solid lines represent the fits to the experimental data.

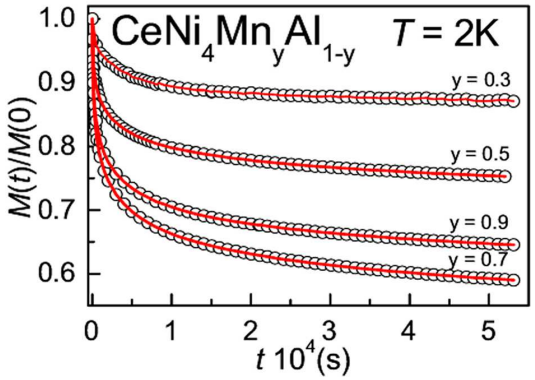

Fig. 7. The magnetic relaxation for the $CeNi_4Mn_yAl_{1-y}$ samples normalized to magnetization in $t = 0$. The solid line is the result of the fitting of the experimental data to $M(T,\,t) = M_0(T,\,0)+\alpha(T)\ln(t+t_s)+\beta\exp((-t+t_s)/\tau)$.

Figure 8 shows a magnetic phase diagram for the $CeNi_4Mn_yAl_{1-y}$ system where T_f has been obtained both from the AC and DC method. In this phase diagram, we define the spin freezing temperature T_f at $f = 10$ kHz of $CeNi_4Mn_yAl_{1-y}$ as the peak temperature in χ'_{AC} curve and as a peak in ZFC χ_{DC} measured at $H = 1$ kOe. T_f changes almost linearly, which is often observed in spin glass systems. The deviations for samples with small amount of Mn can be due to the VF of Ce atoms. The magnetic phase diagram shows mostly a simple transition from the paramagnetic state to SG, which is often observed in Mn containing alloys and compounds [2, 4, 5].

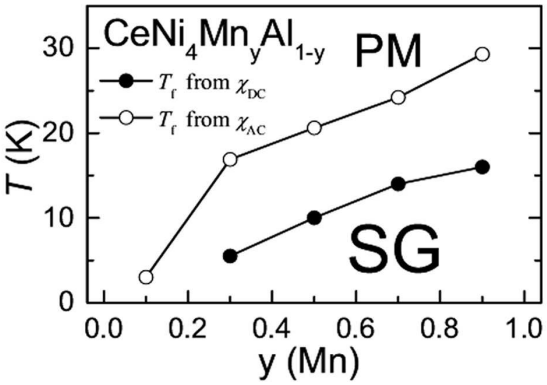

Fig. 8. The magnetic phase diagram for $CeNi_4Mn_yAl_{1-y}$.

4. Conclusions

In conclusion, we have observed the SG behaviour down to 2 K — the lowest temperature used in our studies, for $0 < y < 1$ in the $CeNi_4Mn_yAl_{1-y}$ system, via magnetic properties measurements. Only a small doping with Mn in the place of Al is enough to reveal the SG behaviour. For samples with $y < 0.1$ the SG interaction is suppressed, and the system moves towards regime with VF. The origin of SG is due to the magnetic moments on Mn atoms and due to the disorder on the 3g sublattice in the crystallographic unit cell. The statistical distribution of Mn, Ni and Al atoms introduces the randomly distributed magnetic interactions, which is necessary for formation of the frustration in the SG state.

References

[1] G. Liang, Q. Yao, H. Xi, K. Mochizuki, J.T. Markert, M. Croft, *J. Alloys Comp.* **414**, 8 (2006).

[2] K. Synoradzki, T. Toliński, *J. Phys. Condens. Matter* **24**, 136003 (2012).

[3] G. Liang, F. Yen, *J. Appl. Phys* **103**, 07B719 (2008).

[4] T. Toliński, K. Synoradzki, *Intermetallics* **19**, 62 (2011).

[5] X. Liu, S. Matsuishi, S. Fujitsu, H. Hosono, *Phys. Rev. B* **84**, 214439 (2011).